Hydraulic plasticity and water use regulation act to maintain the hydraulic safety margins of Mediterranean trees in rainfall exclusion experiments

Myriam Moreno, Jean-marc Limousin, Guillaume Simioni, Eric Badel, Jesus Rodríguez-Calcerrada, Hervé Cochard, José Torres-Ruiz, Jean-luc Dupuy, Julien Ruffault, Elena Ormeño, et al.

Hydraulic plasticity and water use regulation act to maintain the hydraulic safety margins of Mediterranean trees in rainfall exclusion experiments

Myriam Moreno[1,2], Jean-Marc Limousin[3], Guillaume Simioni[1], Eric Badel[4], Jesus Rodríguez-Calcerrada[6], Hervé Cochard[4], José M. Torres-Ruiz[4], Jean-Luc Dupuy[1], Julien Ruffault[1], Elena Ormeno[5], Sylvain Delzon[7], Catherine Fernandez[5], Jean-Marc Ourcival[3], and Nicolas Martin-StPaul[1]

[1]INRAE, URFM, Avignon, France

[2]French Environment and Energy Management Agency, Angers, France

[3]CEFE, Univ Montpellier, CNRS, EPHE, IRD, Montpellier, France

[4] Université Clermont Auvergne, INRAE, PIAF, Clermont-Ferrand, France

[5] Aix Marseille Univ, Avignon Université, CNRS, IRD, IMBE, Marseille, France

[6]Research Group Functioning of Forest Systems in a Changing Environment, Universidad Politécnica de Madrid, Spain

[7]INRAE, BioGeCo, Université de Bordeaux, Pessac, France.

* Corresponding author: myriam.moreno@inrae.fr

Key words: hydraulic failure, hydraulic adjustment, phenotypic plasticity, stomatal control, cuticular conductance, turgor, throughfall exclusion, evergreen and deciduous trees.

Abstract:

Hydraulic failure due to xylem embolism has been identified as one of the main mechanisms involved in drought-induced forest decline. The tree vulnerability to hydraulic failure depends on the hydraulic safety margin (HSM), which can be computed as the difference between the highest water stress experienced under drought or turgor loss point and the water stress causing hydraulic failure. While it has been shown that HSM globally converge between tree species and biomes, there is still limited knowledge regarding how HSM can adjust to locally varying drought conditions within species. In this study, we relied on three long-term partial rainfall exclusion experiments in Southern France (15, 9 and 6 years of rainfall exclusion treatment respectively for Puéchabon, Font-blanche and O3HP sites) to investigate the plasticity of hydraulic traits and HSM under intensified drought conditions for three Mediterranean tree species (*Quercus ilex L.*, *Quercus pubescens Willd.,* and *Pinus halepensis Mill.*). Our findings show, for all species, a similar HSM in trees submitted to intensified drought and trees in the control treatments, despite reduced precipitation and, hence soil water availability. This homeostasis of HSM in response to rainfall reduction is achieved through different mechanisms, which appear to be related to the water use strategies of the three species. For *Q. ilex*, our results indicate that the convergence in HSM is attributed to the adjustment of two plant hydraulic traits, namely the turgor loss point (Ψ_{tlp}) and the water potential at which 50% of xylem conductivity is lost due to embolism (P50). In contrast, both *P. halepensis* and *Q. pubescens* exhibited similar minimal water potentials under control and drought treatments, due to isohydric behavior for the first and probably other traits adjustment for the latter. Thus, the plasticity of the hydraulic vulnerability was not required to maintain their HSM in these two species. Our results suggest that trees exposed to moderately drier conditions over several years may be able to maintain plastically their HSM. However, it remains to be seen whether this acclimatization of HSM to drier conditions will be sufficient to withstand the more extreme droughts expected in the Mediterranean region.

Introduction:

Over the last decades, many studies have been conducted to better understand the mechanisms responsible for tree dieback following severe water stress (Barigah et al., 2013; Choat et al., 2018; Sperry et al., 2002; Tyree & Sperry, 1988). Among the different processes involved in plant mortality under drought (Allen et al., 2015; Anderegg et al., 2015), hydraulic failure has been identified as one of the key triggers of tree death (Adams et al., 2017; Anderegg et al., 2016; Arend et al., 2021;

McDowell et al., 2008). During drought, soil and atmospheric drying result in an increase in xylem water tension (i.e., a decrease in plant water potential). Excessive water tension promotes the occurrence of xylem cavitation, which cause the rupture of water columns between roots and leaves by embolism. Hydraulic failure occurs when the water transport in the plant is severely impaired by embolism (Tyree & Sperry, 1989), causing different damages to living tissues that may prevent the recovery of the tree when drought ends, and eventually kill the tree (Mantova et al., 2022).

The timing and likelihood of hydraulic failure during drought is influenced by various physiological characteristics that control plant desiccation resistance (Choat et al., 2018; Duursma et al., 2019; Ruffault et al., 2022). The xylem vulnerability to cavitation is a crucial trait that define the rate of spread of embolism with water potential decrease. It is derived from vulnerability curves relating increased xylem embolism (e.g. the loss of hydraulic conductance) with decreasing xylem water potentials (Cochard, 2002; Cochard et al., 2008, 2013). The main parameter of this vulnerability curve is the water potential causing 50 % of hydraulic conductance loss (P50), which is negatively correlated with survival time during drought and the dryness of species habitat (Lens et al., 2016; Martin-StPaul et al., 2017). The rate of water potential decline during drought (i.e. plant desiccation dynamics resistance) depends, among other factors, on water loss regulation through stomatal control (Martin-StPaul et al., 2017). Thus, the earlier the stomata close after the drought onset, the more the plants are able to limit the decrease in their water potential, and preserve xylem conduits from cavitation. The water potential at turgor loss point (Ψ_{tlp}) can be used as a surrogate of the water potential at which stomata close (Brodribb & Holbrook, 2003; Martin-StPaul et al., 2017), given that stomata close once guard cells lose turgidity. In addition, plant residual transpiration, occurring through incompletely closed stomata or the cuticle (Machado et al., 2021), also determine the rate of the plant-drying process and the hydraulic risk (Duursma et al., 2019).

The hydraulic safety margin (HSM) is an integrative trait used to evaluate the risk of hydraulic failure under drought, with a higher HSM indicating a lower risk. Two versions of HSM have been proposed. The first one corresponds to the difference between the minimum xylem water potential (e.g. $\Psi_{midd\ min}$) reached by a plant and the threshold water potential causing severe xylem embolism (e.g. P50) (Choat et al., 2012). According to this definition, HSM represents the hydraulic risk associated to the water stress actually experienced by the plant. In the second definition, $\Psi_{midd\ min}$ is replaced by the water potential causing stomatal closure (Martin-StPaul et al., 2017). This second version of HSM integrates the degree to which stomatal control can prevent hydraulic risk. Since the minimum potential achieved by a plant depends on stomatal control, the two definitions of HSM are closely linked. The HSM has been shown to be conserved across forest tree species worldwide (Choat

et al., 2012), as a result of the coordination of multiple traits optimizing the xylem safety-efficiency trade-off with species habitat (Franklin et al., 2022; Guillemot et al., 2022; Martin-StPaul et al., 2017; Pivovaroff et al., 2018). However, there has been little investigation into the intraspecific variations of the HSM in response to drier conditions. To our knowledge, the only publication focusing on this topic report narrower HSM for Mediterranean species occurring at the dry edge of their geographical distribution (Alon et al. 2023).

Understanding the impact of plant trait plasticity on plant desiccation dynamics is therefore crucial for predicting hydraulic risk in the current context of rapid climate change (Jinagool et al., 2018). Yet, limited research has thus far investigated the adjustment of multiple traits after long periods of increased drought. Some studies suggested that leaf traits, such as Ψ_{tlp} change more in response to sustained drought than the xylem vulnerability to cavitation (Bartlett et al., 2012; Torres-Ruiz et al., 2019), which is sometimes invariant (Lobo et al., 2018; Rosas et al., 2019) and sometimes plastic (Bert et al., 2021; Herbette et al., 2021; Lemaire et al., 2021). For the Mediterranean species *Quercus ilex*, past studies have reported limited plasticity of xylem vulnerability to cavitation (Limousin et al., 2022; Limousin et al., 2010; Martin-StPaul et al., 2013). Additionally, it is important to note that, until recently, the methods used to measure xylem vulnerability to cavitation in long-vessel branches, such as those of *Q. ilex*, were affected by a bias due to open vessel methodological artefact (Martin-StPaul et al., 2014; Torres-Ruiz et al., 2014). Similarly, the methods used to estimate leaf hydraulic vulnerability curves based on leaf hydraulic conductance were also biased by the integration of an extra-xylary water pathway (Li et al., 2020; Limousin et al., 2022; Trifiló et al., 2016). Hence, it is important to revisit the impact of plant trait plasticity on plant desiccation dynamics with up-to-date and unbiased methods, such as Cavitron (Cochard et al. 2002) or optical vulnerability (Brodribb et al. 2016) techniques.

In this study, we aimed to assess whether, and by which mechanisms, the HSM of a given species can change with increasing drought conditions. We focused on three of the most widespread tree species in the Mediterranean basin, namely *Pinus halepensis Mill.*, *Quercus ilex L.* and *Quercus pubescens Willd.* Those species are being monitored in three long term partial rainfall exclusion experiments set up in natural forests in southern France: the Puéchabon experimental site (a *Q. ilex* forest), the Oak Observatory at the Haute-Provence Observatory (a *Q. pubescens* forest), and the Font-blanche site (a mixed forest of *P. halepensis* and *Q. ilex*). In those three sites, we measured and compared hydraulic traits in adults of the three species under control and aggravated drought conditions.

Materials and Methods:

Sites description

The study was conducted on three experimental forest sites located in the French Mediterranean region (Figure 1A) that stand out by their vegetation types: the Font-blanche (FB hereafter) forest is composed of *P. halepensis* in the overstory and *Q. ilex* in the understory, the oak observatory at the Haute-Provence Observatory (O_3HP hereafter) is dominated by *Q. pubescens*, and the Puéchabon site (P hereafter) by *Q. ilex*. The climate of the sites is Mediterranean, with wet, mild winters and dry, hot summers (Fig. S1). The subsoil of all sites is composed by a hard limestone bedrock. The soils of the FB and P sites are similar and classified as silty clay loam, while the O3HP site is a clay-loam soil. They have a high proportion of rocks and soil depth varies between 35 to 50 in FB and P and 30-40 cm in O_3HP. On all sites, a rainfall exclusion experiment has been implemented for for several years (15, 9 and 6 years respectively for Puéchabon, Font-blanche and O_3HP sites at the time of this study (more details provided in Table 1) excluding approximately 30 % of the precipitation reaching the ground. At FB and P, the system excluding precipitation is passive, with PVC gutters hung under the tree canopies. At O_3HP, rainfall exclusion is achieved with a mobile rainout-shelter deployed manually only during some rainfall events from spring to autumn (Fig. 1). Table 1 provide more details on sites characteristics and rainfall exclusion treatments. On each site, meteorological variables are monitored (including half-hourly precipitation, radiation, air temperature and humidity).

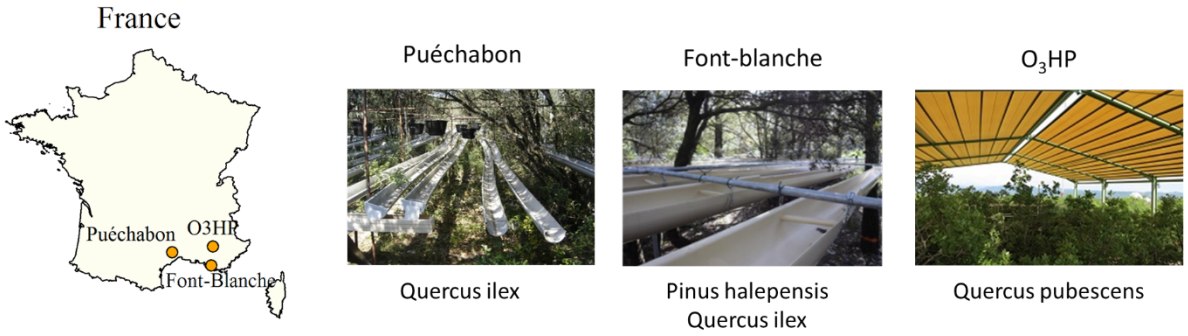

Figure 1. Locations of studied sites and pictures of the rainfall exclusion systems. PVC gutters placed under the canopy were used to collect around 30 % of precipitation at Puéchabon and Font-blanche sites, while in the O_3HP site, a mobile shelter placed above the canopy is deployed manually.

Table 1: Characteristics of studied sites.

	Font-Blanche	**Puéchabon**	**O_3HP**
Location	43°14’27”N, 5°40’45”E	43°44’29”N, 3°35’45”E	43°56′115″ N, 05°42′642″ E

Precipitation (mm) / temperature (°C) (annual mean value between 2016-2019)	615 /14.2	1033 /14.0	871 /12.9
Soil characteristics: type, depth (cm), available soil water (mm)	Silty clay loam, 20 to 50, 160	Silty clay loam, 30 to 70 ,140	Clay-loam, 30 to 40, NA
Vegetation type	Evergreen *P. halepensis* and *Q. ilex* forest	Evergreen *Q. ilex* forest	Deciduous *Q. pubescens* forest
Basal area (m^2/ha) (mean 2018)	29.7	27.2	21
Tree height (mean 2018)	13.5 for *P. halepensis* 6.5 for *Q. ilex*	5.5	5
Rainfall exclusion device, treatments area (m^2), year of the start of the exclusion	Gutters, 625, 2009	Gutters, 140*4 replicates, 2003	mobile rainout-shelter, 300, 2012
Precipitation exclusion ratio	≈ 30 %	≈ 30 %	≈ 30 %
References	(Moreno et al., 2021)	(Limousin et al., 2009)	(Genard-Zielinski et al., 2018)

Water potentials in the field

Water potentials data were taken from Moreno et al. (2021) for *P. halepensis* and *Q. ilex* at FB, from Limousin et al. (2022) for *Q. ilex* at P, and from Genard-Zielinski et al. (2018) for *Q. pubescens* at O_3HP. Predawn (Ψ_{pd}) and midday (Ψ_{midd}) water potentials were measured from 2015 to 2019 in each site (Table 2) during summer using Scholander pressure chambers (different brands depending on year and site). The samplings were performed at several dates from the onset to the end of summer (between two to six measurements per year depending on year and site). At each site and date, measurements were made on twigs (FB and P sites) or leaves (O_3HP site) of at least three trees per species and per treatment (control/ rainfall exclusion). One to three samples per tree were measured depending on site and date during the two hours preceding sunrise for Ψ_{pd}, and between 2 to 4 pm for Ψ_{midd}. Ψ_{midd} were measured on transpiring twigs/leaves. For Ψ_{pd}, we have selected the data from the

date when the lowest values were recorded per species for each year to compute the extreme annual predawn water potentials ($\Psi_{pd\ min}$). For Ψ_{midd}, we have selected the data from the date when minimum values were observed, combining all years, to compute the extreme midday water potentials ($\Psi_{midd\ min}$).

Vulnerability to cavitation

Depending on the length of xylem conduits of each species, two techniques were used to measure the xylem vulnerability to cavitation. For *P. halepensis*, a gymnosperm species with only tracheids, we used the cavitron technique (Cochard, 2002). In March 2018 and October 2019, south facing branches, approximatively 50 cm long, were sampled from the top of the canopy of a total of 17 control trees and 10 trees submitted to rainfall exclusion of the FB site (Table S1: no significant difference of P50 between sampling date, Fig. S2). Once cut, branches were placed under water and the basal 10 cm recut to eliminate cavitated tracheids due to conduits left open during the first cut. Then, they were placed in humidified black bags in order to limit transpiration and prevent dehydration. At the laboratory, branches were placed under water, the foliage was removed, and a straight 30-cm-long section of the branch was recut. The sections were rolled into humidified absorbent paper, wrapped in plastic film, and placed in an icehouse for shipping them to the to the INRAE-PIAF laboratory at Clermont-Ferrand (central France). There, the bark was removed and the vulnerability to cavitation of the samples measured with the cavitron (Cochard, 2002). Tension in the xylem was gradually increased, with the rotation speed and the percent loss of conductivity (PLC) being calculated using Cavisoft (v.4.0; University of Bordeaux) as:

$$PLC\ (\%) = 100*(1-K/K_{max}) \quad (1)$$

where K is the conductivity recorded at a given rotation speed and K_{max} the maximal conductivity recorded at the lowest rotation speed.

Xylem vulnerability curves were then constructed for each sample by plotting PLC as a function of the xylem tension caused by rotation. The following sigmoid function was fitted to data:

$$PLC = 100/\ (1+\exp(s(P-P50))) \quad (2)$$

where s is the slope at the inflexion point and P50 is the water potential causing 50 % loss of hydraulic conductivity.

Because xylem vessel length in the two oaks species can reach up to 1m (Martínez-Vilalta et al., 2002), we were unable to employ the cavitron technique with oaks, due to the bias for long-vessel

species when branch samples are shorter than the vessel length (Beikircher et al., 2010; Cochard et al., 2013; Martin-StPaul et al., 2014; Sergent et al., 2020). Instead, we used the optical technique (Brodribb et al., 2016) to measure the xylem vulnerability to cavitation in the leaves. We opted for the leaf optical technique rather than the stem optical technique, as it does not require to remove tissue limiting potential bias caused by endommaged xylem if not well executed. All the branches used to measure VC were not flushed to remove native embolism, as such procedure can bias vulnerability curves (https://doi.org/10.1093/treephys/tpad088) due to open-vessels artifact. Drawing from the findings of Li et al., (2020), and our own observation of similar P50 using the optical method and respectively X-ray microtomography for *Q. ilex* stems (Sergent et al, 2020) and cavitron for *Q. pubescens* branches (personal data given by Delzon) (Fig. S3), we assumed that hydraulic segmentation did not occur in the two oak species. Anyway, despite the use of different hydraulic techniques across species, it is important to note that the aim of this study is to evaluate intraspecific plasticity in hydraulic traits, rather than interspecific drought tolerance.

During summer 2019, 4 to 5 branches more than 1 m long of *Q. ilex* and *Q. pubescens* sampled from different trees, were harvested in each control and rainfall exclusion treatments of the three studied sites. Branches were placed in humidified bags and stored in a dark cold room with the cut end in water for at least one night to rehydrate. Once fully rehydrated, branches were allowed to dehydrate progressively on the lab bench (bench dehydratation technique). One or two mature leaves per branch, still attached to the branch, were placed on a flatbed light transmission scanner (Epson V850). The leaves were kept flat using microscope slides attached to the scanner glass with transparent tape. Leaf scans of a resolution of 2400 dpi were recorded in light transmission mode every 5 min while the branch was progressively dehydrating. Concomitantly, xylem water potential was measured on bagged leaves of the same branch using a Scholander pressure chamber (PMS instrument), approximatively every 3 hours throughout branch desiccation (along 3 to 5 days, a minimum period of 3 days being enough to reach 100% emboli in the xylem, Fig. S4).

Once the branch fully desiccated (and the xylem water potential was no longer measurable with Scholender pressure chamber), all images were analyzed to detect cavitation events as changes in light transmittance between successive scans (http://www.opensourceov.org/). Image J (FIJI, (Schindelin et al., 2012)) was used to reveal embolism events by overlapping successive leaf scans and calculating the pixel area of embolized vessels. Vulnerability curves were constructed for each leaf by plotting the relative cumulative embolized area (corresponding to the cumulative embolized area divided by the total embolized area at the end of leaf dehydration) as a function of leaf water potential, and fitting the same sigmoid function as for *P. halepensis*.

Foliar traits

Pressure–volume curves (hereafter PV curves) were used to characterize different foliar traits related to the maintenance of leaf turgor and hydration (Bartlett et al., 2012; Tyree & Hammel, 1972). For each species, two well-lit twigs per tree were collected from the outer crown of 4-6 trees in the control and exclusion treatments. The sampling took place in March 2018 for *P. halepensis* and *Q. ilex* at FB and P sites and in September 2019 for *Q. pubescens* at O_3HP site. In all cases, once collected, twigs were bagged and placed in a cooler at 4°C until reaching the laboratory. Once in the lab, each twig end was re-cut under water with a razor blade, then put overnight in a cool chamber in distilled water to rehydrate. Half of the samples were used to estimate the leaf mass area and the other half to perform the PV curves

PV curves were established using the bench drying method proposed by Hinckley et al., (1980). Briefly, the weight and the water potential of the twigs were measured all along their dehydration using a precision balance (FS-220, resolution 0.1 mg) and a Scholander pressure chamber (PMS instrument), respectively. To overcome oversaturation of rehydrated twigs, the first measurement of water potential and weight was removed, and full turgor weight was extrapolated from the regression between twig weight and water potential before the turgor loss point. The osmotic potential at full turgor (π_{100}) and at the turgor loss point (Ψ_{tlp}), the relative water content at turgor loss point (RWC_{tlp}), the symplastic water fraction at full turgor (Fs), and the bulk modulus of tissue elasticity (ε) were obtained by plotting the inverse of water potential (-1/ Ψ, in MPa) against twig water saturation deficit (1-Relative Water Content, in %). PV curves data used for *Q. ilex* are the same as those reported in Limousin et al. (2022).

Minimum leaf conductance to water vapor (g_{min}) was obtained considering the average twig water loss (corresponding to sample transpiration) after stomatal closure. To this end, relative humidity and temperature were recorded every second with a probe (PT100) to compute VPD, and minimum leaf conductance was obtained as follows for each species:

$$g_{min} = \frac{E}{VPD \times DA} \times Patm, \quad (3)$$

with E being the transpiration after turgor loss, Patm the atmospheric pressure (set at 101 kPa), and DA the developed leaf area. The developed leaf area (DA) was obtained from the projected leaf area by using the ratio between leaf dry mass and leaf mass per area. For both oaks, with flat leaf surface, DA was calculated as twice the projected leaf area. For *P. halepensis*, we calculated DA considering

that needles formed a perfect half-cylinder, which was confirmed by measurements of width and thickness at the top, middle and bottom of 15 needles (data not shown). We choose to express gmin in function of developed leaf area to report more realistic value. Indeed, gmin does not result only from water loss through not fully close stomata but also by cuticular leaks, that can happen from all the leaf surface.

Hydraulic safety margins

Two types of Hydraulic safety margins (HSM) were computed at each site and for both treatments by subtracting either (i) the minimal midday water potentials ($\Psi_{midd\ min}$) to P50, following the approach outlined by Choat et al. (2012), or (ii) the tugor loss point, as a surrogate as water potential causing stomatal closure to P50 as in Martin-StPaul et al. (2017).

To avoid damaging trees, the samples collected to construct hydraulic vulnerability curves were taken from different trees than those sampled for leaf water potential and turgor loss point measurements. Therefore, it was not possible to calculate the HSM at the tree level. Instead, we determined both HSM versions at the species and treatment levels using a nonparametric bootstrap approach. For each species and treatment (control and rainfall exclusion), we randomly sampled, with replacements, 5 values of P50 and $\Psi_{midd\ min}/\Psi_{tlp}$ and determined 5 HSM as the difference between these values. This process was repeated 1,500 times to obtain a distribution of HSM values for each site and treatment that was subsequently used for statistical comparisons.

Native stem xylem embolism measured by X-ray microtomography

Native stem xylem embolism was estimated for *Quercus ilex* and *Pinus halepensis* trees in both rainfall exclusion and control treatments at FB and P. The sampling took place in March 2018. Four to eight well-lit branches of more than 1m were collected depending on the sites, the treatments and the species considered. Once collected, branches were immediately recut under water to avoid cutting artefacts.

The cut surface of the branches was kept under water until reaching the laboratory. Then, short segments of branches (diameter < 0.7 cm and length < 4 cm) were cut under water, plunged in liquid paraffin, and stored in a cold chamber at 4°C until analysis. Measurements were performed following the protocol described in Cochard et al. (2015). Samples were inserted in an X-ray microtomograph (Nanotom 180 XS; GE, Wunstorf, Germany) and analyzed using a field of view of 5 × 5 × 5 mm^3, X-

ray voltage of 60 kV, current of 240 µA, and a scan time of 21 min. The final spatial resolution of the 3D images was 2.5 µm after 3D-reconstruction. For each sample, one transversal 2D slice was extracted from the middle of the branch using VGStudio Max© software (Volume Graphics, Heidelberg, Germany). The surface area of embolized conduits was estimated from slices using the software ImageJ (Schneider et al., 2012).

As *Q. ilex* is a semi ring-porous species with log normal distribution of xylem conduit sizes, we measured the surface area of large embolized vessels (contributing the most to hydraulic conductivity) to estimate their mean diameter and their corresponding hydraulic conductivity. The maximal hydraulic conductivity was estimated thanks to a second scan we performed on the same branch sample once it was fully embolized. The level of embolism was calculated as the ratio between estimated native hydraulic conductivity and maximum hydraulic conductivity.

Table 2. Summary of measurement periods according to sites and species. FB and P are the acronyms for respectively Font-Blanche and Puéchabon sites.

Measurements	***P. halepensis***	***Q. pubescens***	***Q. ilex FB***	***Q. ilex P***
Trees water potentials $\Psi_{pd\ min}$ (MPa)	From 2013 to 2018	2014, 2015, 2018	From 2013 to 2018	From 2015 to 2018 2017
$\Psi_{midd\ min}$ (MPa)	2018	2015	2017	2017
Pressure volume curves: Ψ_{tlp} (MPa), π100(MPa)	March 2018	September 2019	March 2018	March 2018
g_{min} (mmol s^{-1} m^{-2})	March 2018	September 2019	March 2018	March 2018
Xylem vulnerability to cavitation: P50 (MPa)	March 2018, October 2018	September 2019	Onset of summer 2019	Onset of summer 2019
Native stem xylem embolism (%)	March 2018	/	March 2018	March 2018

Statistics

To assess whether plant and leaf traits were different between treatments we used t-test for all traits measured. For the HSM, we made a Student t-test for each of the 1500 subsamples obtained via bootstrapping. We considered that rainfall exclusion and control treatments were significantly different if the probability of having a P_value > 0.05 among the 1500 t-tests realized was lower than 0.05. Statistical analyses were performed with the R software (3,5,2, R Development Core Team 2018). Differences in parameters derived from xylem vulnerability curve (slope and P50; Table S2-3, Fig S5), π100, Ψ_{tlp} or g_{min} between rainfall exclusion and control treatments were found to be similar for *Q. ilex* in both Font-blanche and Puéchabon sites (Limousin et al., 2022). Hence, to

increase the statistical power in testing for a rainfall exclusion effect on traits values, as in Limousin et al. (2022) we decided to combine the data from both sites for this particular species. All Statistical analyses were performed with R software (3,5,2, R Development Core Team 2018)

Results

Rainfall exclusion impacts on tree water status

Variations in the response of $\Psi_{pd\ min}$ to rainfall exclusion treatments were observed among different tree species and sites (Fig. 2). For *Q. pubescens* at O_3HP, $\Psi_{pd\ min}$ tended to be more negative for trees growing in the rainfall exclusion treatments (P_value = 0.005) until 2015 (two years after the onset of the rainfall exclusion). After that, $\Psi_{pd\ min}$ was similar to that of control trees (P_value > 0.1). For *P. halepensis* at FB, $\Psi_{pd\ min}$ were similar across years, except in 2015 (P_value = 0.05), when they were slightly more negative in the rainfall exclusion treatments (Fig. 2). It should be noted, however, that if we consider the whole water potential dynamic rather than the extreme values, significantly more negative potentials in rainfall exclusions appear between treatments at lower levels of water stress (Genard-Zielinski et al., 2018; Moreno et al., 2021). Moreover, soil water content taken at shallow ground level (< 50 cm), tended to be more negative in the rainfall exclusion treatment than in the control (Genard-Zielinski et al., 2018; Moreno et al., 2021). All of these findings attest to the effectiveness of the exclusion treatments for these two species.

Concerning *Q. ilex* at both FB and P sites, $\Psi_{pd\ min}$ tended to be more negative in the rainfall exclusion treatments (Fig. 2, P_value < 0.05 in FB site until 2015; P_value < 0.006 in P site until 2016, then P_value < 0.05).

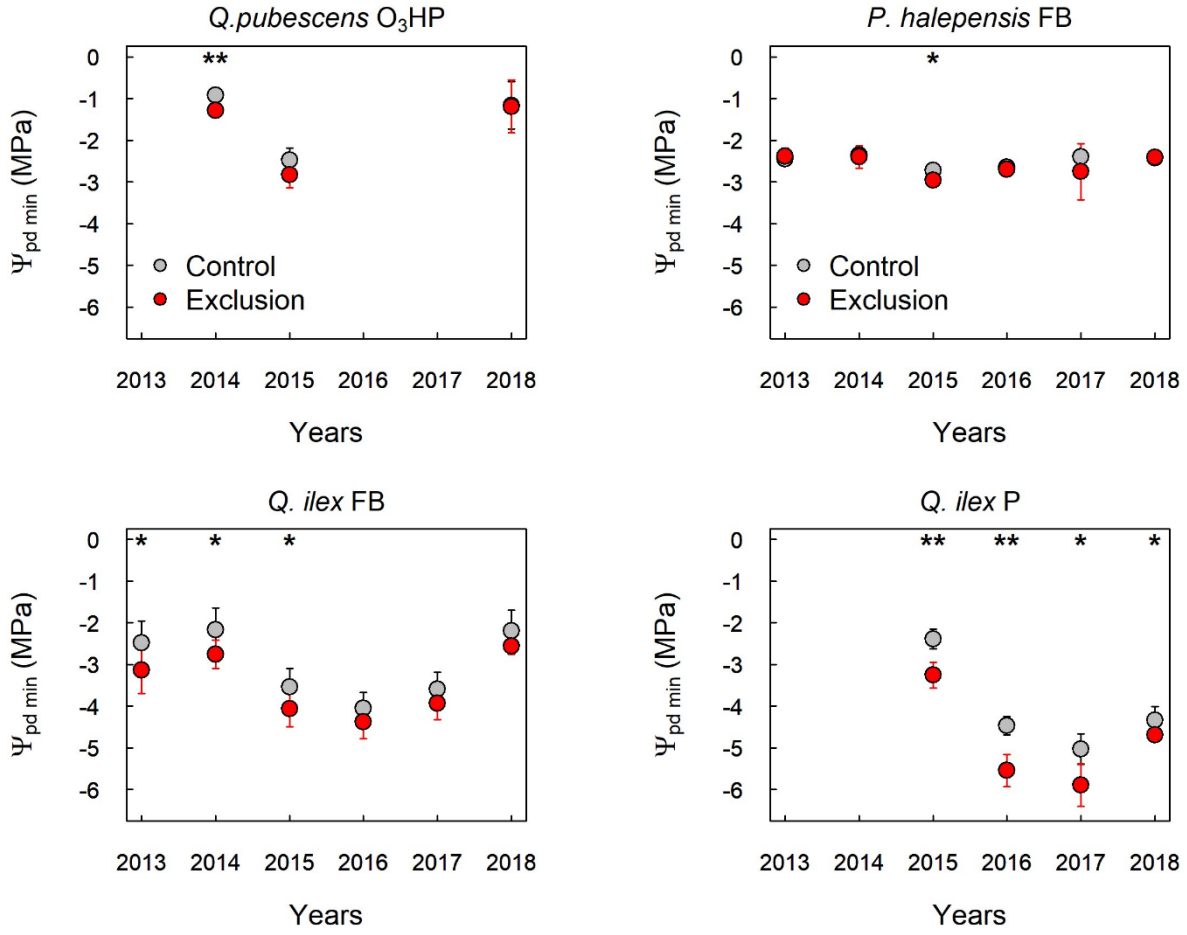

Figure 2. Average minimum predawn water potentials ($\Psi_{pd\ min}$) measured for each species in both control and rainfall exclusion treatments according to year and site. Bars represent standard deviations associated to the mean. Significant differences between treatments (t-test) are indicated by asterisks (*, 0.01 ≤ P_value < 0.05; **, 0.001 ≤ P_value < 0.01; ***, P_value < 0.001).

Effects of rainfall exclusion on hydraulic and leaf traits

No significant differences in P50, π_{100}, Ψ_{tlp} nor g_{min}, were found between the rainfall exclusion and control treatments for *Q. pubescens* and *P. halepensis* (Fig. 3, P_value > 0.2 for each of these traits). For *Q. ilex*, P50, π_{100} and Ψ_{tlp} were significantly more negative for trees growing in the rainfall exclusion (P_value = 0.04 for P50; P_value = 0.02 for $\pi_{100;}$ P_value = 0.03 for Ψ_{tlp}), whereas g_{min} remained unchanged (P_value > 0.05).

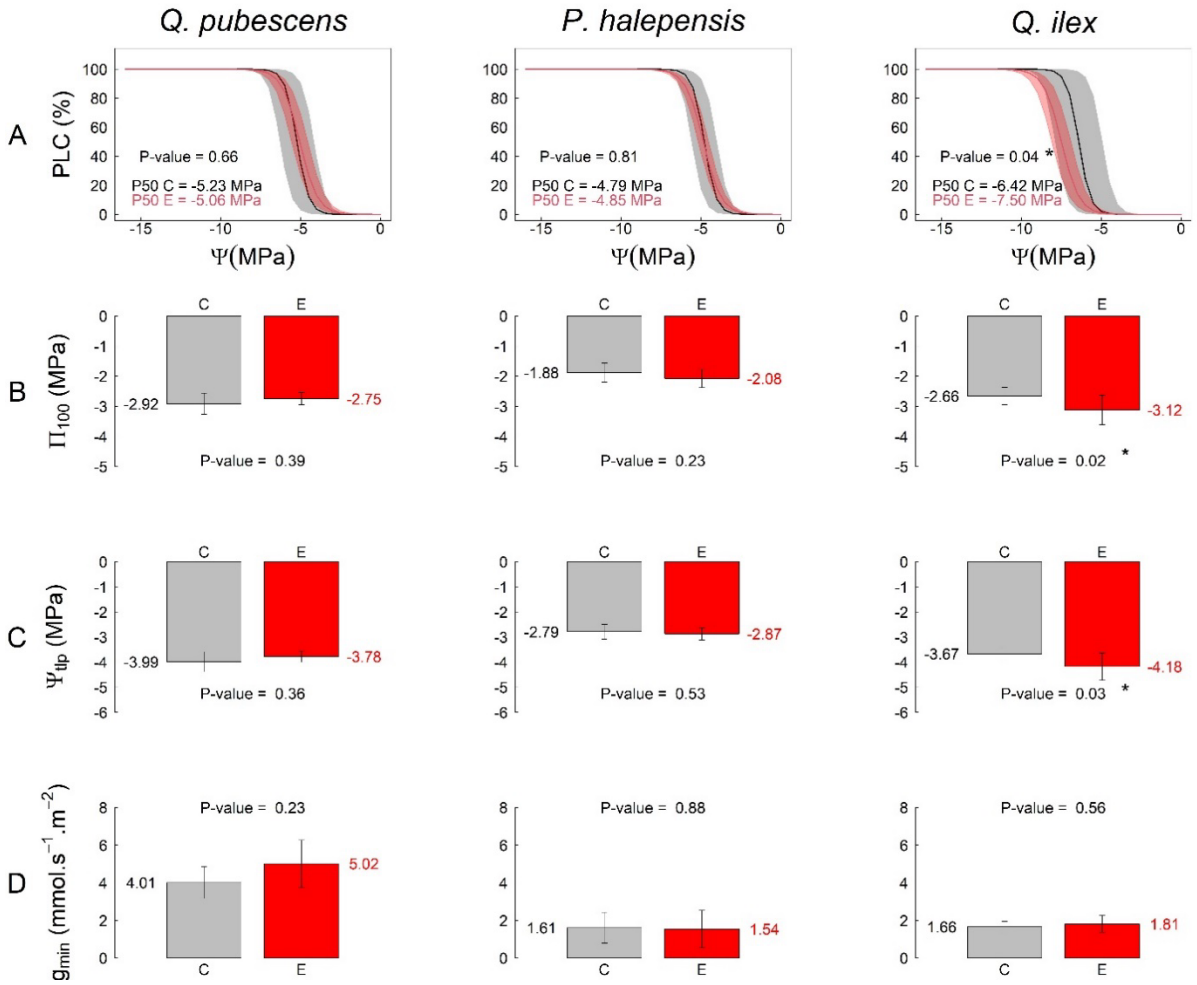

Figure 3. Effects of rainfall exclusion on hydraulic traits for the three studied species. A. Xylem vulnerability curves to cavitation, represented by the percent loss of conductivity (PLC) as a function of water potential (Ψ). Averages and standard deviations are respectively in bold lines and grey (control) or red (rainfall exclusion) areas. B. Osmotic water potential at full turgor (π_{100}), C. water potential at turgor loss point (Ψ_{tlp}), D. minimum leaf conductance (g_{min}) in the control (C, in grey) and rainfall exclusion (E, in red) treatments, for the three studied species. In the barplots, bars represent mean values; error bars represent standard deviation. P_values of treatment effect are presented; asterisks indicate a significant difference at P_value < 0.05.

Effect of rainfall exclusion on species hydraulic safety margins and xylem embolism.

For all species, we did not observe any statistical difference in HSM between rainfall exclusion and control trees, based on either $\Psi_{midd\ min}$ (Fig. 4A, P_value > 0.8 for each species) or Ψ_{tlp} (Fig. 4B, P_value > 0.9 for each species). Levels of native stem xylem embolism were also similar in both treatments for *P. halepensis* or *Q. ilex*, the only species analyzed (Fig. 5).

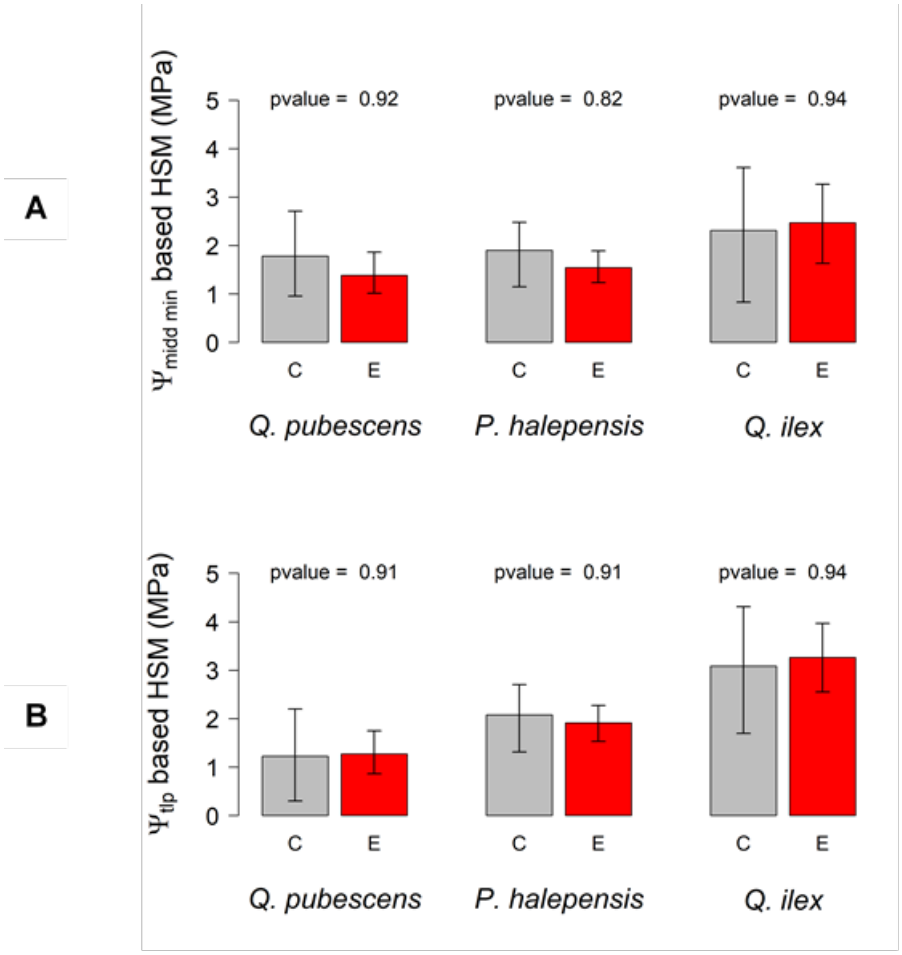

Figure 4. A. Hydraulic safety margins (HSM) in relation to species and treatment (C: control; E: rainfall exclusion). A. HSM defined as the difference between minimum midday water potentials ($\Psi_{midd\ min}$) and water potential causing 50% loss of hydraulic conductivity (P50). $\Psi_{midd\ min}$ correspond to the minimal values measured in 2015 for *Q. pubescens*, 2016 for *Q. ilex* in P and FB sites and 2018 for *P. halepensis*. B. HSM defined as the difference between turgor loss point (Ψ_{tlp}) and P50. Bars and errors bars represent respectively the median and the first/third quartiles (confidence interval) of the nonparametric bootstrap analysis.

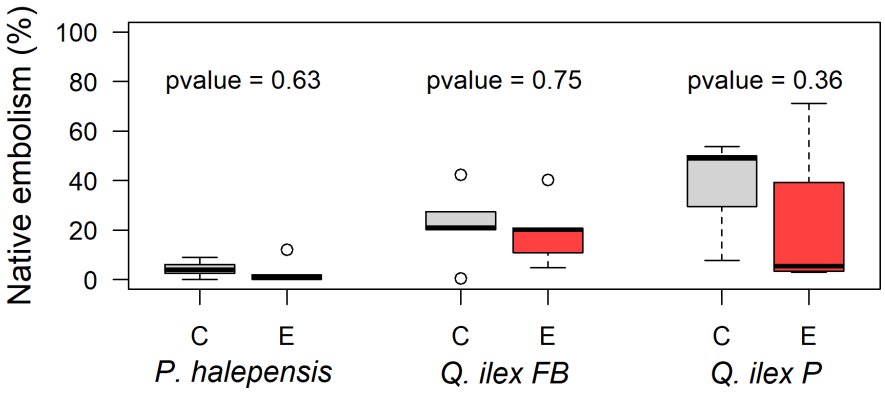

Figure 5. Native stem xylem embolism (%) estimated from X-ray microtomography on 4 years-old branches of *P. halepensis* and *Q. ilex* trees from the control (C) and rainfall exclusion (E) treatments at both Font-blanche (FB) and Puéchabon (P) sites. The measurements were performed in March 2018. P_value of Wilcoxon rank sum tests comparing native stem xylem embolism between treatments are represented for both sites.

Discussion

In the current context of rapid global change, tree capacity to acclimate to increasing drought appears crucial for the maintenance of forest structure, composition and function. Under drier conditions, hydraulic failure risk should increase for trees if they cannot adjust key hydraulic traits involved in the hydraulic safety. In the present study, we aimed to prospect the ability of three functionally different species (different drought response strategies, clades, phenology, etc.) to modify these traits under increasing drought conditions, and to assess the hydraulic risk ensued. Among the three studied species, only *Q. ilex* exhibited significant plasticity in the hydraulic traits prospected, but all three species maintained the hydraulic safety margins (HSM). In the following, we first discuss the effects of the hydraulic adjustments of *Q. ilex* for its drought tolerance capacity. Then, we argue about the likely causes leading to a lack of hydraulic adjustment under rainfall exclusion treatment for both *P. halepensis* and *Q. pubescens*. Finally, we discuss the consequences of HSM homeostasis in response to drier conditions across species for their hydraulic risk.

Homeostasis of HSM due to plasticity in *Q. ilex*

Q. ilex reached lower values of both $\Psi_{pd\ min}$ and $\Psi_{midd\ min}$ in the rainfall exclusion treatments of both FB and P sites (Fig. 2, S6). Thus, the higher water stress experienced by this species in response to increased drought could be the trigger for P50 and Ψ_{tlp} adjustments towards more negative values (Fig. 3, S7).

Until now, studies focusing on long-term drought acclimation of *Q. ilex* had concluded that no plasticity of hydraulic vulnerability occurred for adult trees undergoing rainfall exclusion, in either branches (Limousin et al., 2010; Martin-StPaul et al., 2013) or in leaves (Limousin et al. 2022). Our results contradict those previous works. This could be explained by the facts that: 1) previous estimates of P50 in the xylem of branches were possibly biased by the open-vessel artifact (Martin-StPaul et al., 2014; Torres-Ruiz et al., 2014); 2) estimations of xylem vulnerability to cavitation in branches include several wood rings, which may hide xylem plasticity occurring after a specific aggravated drought; and 3) the rehydration kinetics method used to calculate leaf hydraulic conductance may not reflect only the xylem vulnerability to cavitation but also an extra-xylary component in the leaf mesophyll (Li et al., 2020; Limousin et al., 2022; Trifiló et al., 2016). The optical technique (Brodribb et al., 2016) used in this study for *Q. ilex* and *Q. pubescens* appears as a good solution to overcome these limitations. It allows the estimation of hydraulic vulnerability in the xylem only and in leaves, that are shorter lived, and therefore less affected than branches, by the potential biases due to regrowth and cavitation fatigue, or by methodological issues related to the flushing of native stem xylem embolism and vessels open at both ends (Gauthey et al., 2020).

In addition to the adjustment of xylem vulnerability to cavitation, our findings also highlighted that turgor-related traits also changed for this species under aggravated water stress conditions. Indeed, for *Q. ilex* trees growing in the rainfall exclusion treatments, lower π_{100} values were reported (Limousin et al., 2022), that translate into a significant reduction of Ψ_{tlp} (Bartlett et al., 2012). As stomatal closure is realised through the loss of stomata guard cells turgidity, Ψ_{tlp} could be used as a surrogate of the point of stomatal closure (Martin-StPaul et al., 2017). This suggests that *Q. ilex* trees from the rainfall exclusion treatments could close their stomata at lower water potentials than trees from the control treatments thus allowing them to maintain more photosynthetic activity or root growth under similar drought conditions. This adjustment may lead to an increased risk of xylem embolism if the vulnerability to cavitation, P50, is not also reduced. The apparent coordinated plasticities of $\Psi_{tlp,}$ that is lowered by 0.5 MPa, and of P50 that is lowered by 1 MPa, could be beneficial to leaf gas exchange, without affecting the hydraulic safety margin (Fig. 4B). This maintenance of the HSM in spite of drier conditions seems confirmed by the similar levels of native stem xylem embolism observed in the *Q. ilex* trees growing inside the rainfall exclusion treatments and those growing under control conditions (Fig. 5). Limousin et al., (2022) showed that Fs increased significantly in the rainfall exclusion treatments, suggesting that lower Ψ_{tlp} do not result from internal cell water loss but rather from the accumulation of osmolytes. Hence, we can assume that, besides its action on stomatal control, osmotic adjustment in the exclusion treatments could also play a role in

limiting cell dehydration and hence drought-induced damages on leaves, which is crucial for this evergreen species with a leaf lifespan of two to three years (La Mantia et al., 2003).

Regarding the minimal leaf conductance (g_{min}), which is implied in water loss after stomatal closure (Duursma et al., 2019), we observed no plasticity in response to long-term increased drought for *Q. ilex* or any of the other species (Fig. 3). This suggests either that g_{min} is not or little plastic, or that more precise methods, such as the drought box (Billon et al., 2020), should be used to detect plasticity in this trait.

Homeostasis of HSM despite lack of plasticity in *P. halepensis* and *Q. pubescens*

The most likely explanation for the lack of adjustments in hydraulic traits for *P. halepensis* and *Q. pubescens* is that these species experienced similar levels of extreme water stress under both control and rainfall exclusion treatments, and that that was no advantage in increasing HSM. This hypothesis appears plausible for *P. halepensis*, for which $\Psi_{pd\ min}$ were similar between rainfall exclusion and control trees (Fig. 2). Such result is consistent with its behavior in response to drought. Indeed, *P. halepensis* is an isohydric species that strongly regulates its transpiration at the onset of drought, allowing it to limit soil water consumption and maintain both Ψ_{pd} and Ψ_{midd} (Figs. 2, 3) over a safe threshold of -3 MPa (Moreno et al., 2021). Recently, (Moreno et al., 2024) proposed that such isohydric behaviour is the results of two meachnisms : (i) its stomatal closure that happened at relatively high level of water stress and (ii) its ability to isolates itself from the ground and the atmosphere. Hence, its water use strategy seems sufficient in itself to limit hydraulic damages caused by rainfall reduction, without requiring xylem adjustments, at least under our experimental conditions. The fact that native stem xylem embolism were similar between rainfall exclusion and control treatments (Figs. 5, 6) further supports this idea.

For *Q. pubescens*, given its anisohydric behaviour like for *Q. ilex* (Damesin & Rambal, 1995; Poyatos et al., 2008), we expect trees from the rainfall exclusion to be exposed to more negative water potentials. In 2014, two years after the onset of the rainfall exclusion experiment, a significant difference between Ψ_{pd} of control and rainfall exclusion trees was observed. This result attests the effectiveness of the rainfall exclusion, which is in line with the significant reduction in soil moisture measured in the rainfall exclusion treatments (Genard-Zielinski et al., 2015, 2018). Nevertheless, for the following studied years, $\Psi_{pd\ min}$ was similar between treatments. This result, which seems at first

sight contradictory, probably underpins other adjustments in unprospected traits. The figure S8 shows that at the onset of the experiment, the amount of leaf loss by the trees of the rainfall exclusion is 1.5 higher than the one of the control treatment, suggesting highest leaf area index in the rainfall exclusion plot. Throughout the experiment, the gap between the litterfalls of the two treatments narrows to become similar in 2018. This result suggests that trees in the exclusion plot have reduced leaf production and therefore their overall leaf area, limiting overall transpiration and hence water potential decrease. Other adjustment could also occured as, for example, an increase of rooting depth could be induced after aggravated water stress, as proposed by Martin-StPaul et al. (2013), enabling trees to access deeper soil water and thus limiting their drought exposure. Likewise, earlier leaf senescence could also occur in trees facing drier conditions (Wu et al., 2022). These additional adjustments occurring at the whole tree scale could be sufficient to dampen the rainfall exclusion effect on extreme tree water stress and prevent hydraulic damages (Fig. 5). Further investigations are however needed to identify the other traits implied in the homeostasis of hydraulic risk for this species.

The risk of maintaining the HSM for species vulnerability under future climatic conditions.

Although achieved through different means, our data report a maintenance of HSM under experimental 30 % rainfall exclusion (Fig. 4) for the three studied species. This suggest that no matter the drought response strategies adopting by these species, trees exposed to drier conditions adjusted functionally to preserve this trait. One might have expected that, in order to reduce hydraulic risk, trees could have adjusted to increase HSM values, through the development of a more cavitation resistant xylem. A reasonable explanation that could be advanced to explain this lack is the need for the plant to optimize fluxes relative to the hydraulic risk and that can be achieve through a myriad of strategies. The maintenance of HSM in response to plasticity that we reported in this study is in line with metanalysis from Choat et al. (2012), which reports a worldwide convergence of forest vulnerability to drought (estimated through tree HSM) at the interspecific level independently of the level of drought. The fact that trees seem to maintain HSM despite several years of increasing drought calls into question the natural capacity of forests to withstand accelerating climate change. To what extent HSM can be maintained in the future and at what cost, is still an open question. It remains to be known how much future extreme drought or heat waves may affect acclimated and non-acclimated trees. The next step is to use traits based mechanistic process-based models (Martin-StPaul et al.,

2017; Blackman et al., 2019, Ruffault et al. 2023), in order to characterize hydraulic risk in various conditions. In particular, they would enable to assess how the combination of several traits could translate into different levels of risk in a warmer, drier future.

Acknowledgments

The authors thank the Phenobois Plateform (INRAE, Clermont-Ferrand-France) for the observation by X-ray microtomography; Amélie Tournant and Pierre-Jean Dumas for their help in the extraction of data of xylem vulnerability curves; Arnaud Jouineau and Jean-Phillipe Orts for their help in collecting samples and Ilja Reiter for the meteorological data of the O_3hp site The Puéchabon, Font-Blanche and O_3HP experimental sites all belong to the French national research infrastructure ANAEE-France (ANR-11-INBS-0001), with Puéchabon and Font-Blanche also belonging to the French network of ICOS Ecosystem stations (Integrated Carbon Observation System ERIC). Puéchabon is further supported by the OSU OREME (UMS 3282). J. R.-C. acknowledges the "Ministerio de Educación Cultura y Deporte" for a "José Castillejo" mobility grant.

References

Adams, H. D., Zeppel, M. J. B., Anderegg, W. R. L., Hartmann, H., Landhäusser, S. M., Tissue, D. T., Huxman, T. E., Hudson, P. J., Franz, T. E., Allen, C. D., Anderegg, L. D. L., Barron-Gafford, G. A., Beerling, D. J., Breshears, D. D., Brodribb, T. J., Bugmann, H., Cobb, R. C., Collins, A. D., Dickman, L. T., … McDowell, N. G. (2017). A multi-species synthesis of physiological mechanisms in drought-induced tree mortality. *Nature Ecology and Evolution*, *1*(9), 1285–1291. https://doi.org/10.1038/s41559-017-0248-x

Allen, C. D., Breshears, D. D., & McDowell, N. G. (2015). On underestimation of global vulnerability to tree mortality and forest die-off from hotter drought in the Anthropocene. *Ecosphere*, *6*(8). https://doi.org/10.1890/ES15-00203.1

Alon, A., Cohen, S., Burlett, R., Hochberg, U., Lukyanov, V., Rog, I., Klein, T., Cochard, H., Delzon, S., & David-Schwartz, R. (2023). Acclimation limits for embolism resistance and osmotic adjustment accompany the geographical dry edge of Mediterranean species. Functional Ecology, 37, 1421–1435. https://doi.org/10.1111/1365-2435.14289

Damesin, C., & RAMBAL, S. (1995). Field study of leaf photosynthetic performance by a Mediterranean deciduous oak tree (Quercus pubescens) during a severe summer drought. *New Phytologist*, *131*(2), 159–167. https://doi.org/10.1111/J.1469-8137.1995.TB05717.X

Anderegg, W. R. L., Hicke, J. A., Fisher, R. A., Allen, C. D., Aukema, J., Bentz, B., Hood, S., Lichstein, J. W., Macalady, A. K., Mcdowell, N., Pan, Y., Raffa, K., Sala, A., Shaw, J. D., Stephenson, N. L., Tague, C., & Zeppel, M. (2015). Tree mortality from drought, insects, and their interactions in a changing climate. *New Phytologist*, *208*(3), 674–683. https://doi.org/10.1111/NPH.13477

Anderegg, W. R. L., Klein, T., Bartlett, M., Sack, L., Pellegrini, A. F. A., Choat, B., & Jansen, S. (2016). Meta-analysis reveals that hydraulic traits explain cross-species patterns of drought-induced tree mortality across the globe. *Proceedings of the National Academy of Sciences of the United States of America*, *113*(18). https://doi.org/10.1073/pnas.1525678113

Arend, M., Link, R. M., Patthey, R., Hoch, G., Schuldt, B., & Kahmen, A. (2021). Rapid hydraulic collapse as cause of drought-induced mortality in conifers. *Proceedings of the National Academy of Sciences of the United States of America*, *118*(16). https://doi.org/10.1073/pnas.2025251118

Barigah, T. S., Charrier, O., Douris, M., Bonhomme, M., Herbette, S., Améglio, T., Fichot, R., Brignolas, F., & Cochard, H. (2013). Water stress-induced xylem hydraulic failure is a causal factor of tree mortality in beech and poplar. *Annals of Botany*, *112*(7). https://doi.org/10.1093/aob/mct204

Bartlett, M. K., Scoffoni, C., & Sack, L. (2012). The determinants of leaf turgor loss point and prediction of drought tolerance of species and biomes: A global meta-analysis. *Ecology Letters*, *15*(5), 393–405.

Beikircher, B., Ameglio, T., Cochard, H., & Mayr, S. (2010). Limitation of the Cavitron technique by conifer pit aspiration. *Journal of Experimental Botany*, *61*(12), 3385–3393. https://doi.org/10.1093/JXB/ERQ159

Bert, D., Le Provost, G., Delzon, S., Plomion, C., & Gion, J. M. (2021). Higher needle anatomic plasticity is related to better water-use efficiency and higher resistance to embolism in fast-growing Pinus pinaster families under water scarcity. *Trees - Structure and Function*, *35*(1), 287–306. https://doi.org/10.1007/S00468-020-02034-2

Billon, L. M., Blackman, C. J., Cochard, H., Badel, E., Hitmi, A., Cartailler, J., Souchal, R., & Torres-Ruiz, J. M. (2020). The DroughtBox: A new tool for phenotyping residual branch conductance and its temperature dependence during drought. *Plant, Cell & Environment*, *43*(6), 1584–1594. https://doi.org/10.1111/PCE.13750

Brodribb, T. J., & Holbrook, N. M. (2003). Stomatal closure during leaf dehydration, correlation with other leaf physiological traits. *Plant Physiology*, *132*(4). https://doi.org/10.1104/pp.103.023879

Brodribb, T. J., Skelton, R. P., Mcadam, S. A. M., Bienaimé, D., Lucani, C. J., & Marmottant, P. (2016). Visual quantification of embolism reveals leaf vulnerability to hydraulic failure. *New Phytologist*, *209*(4), 1403–1409. https://doi.org/10.1111/NPH.13846

Choat, B., Brodribb, T. J., Brodersen, C. R., Duursma, R. A., López, R., & Medlyn, B. E. (2018). Triggers of tree mortality under drought. In *Nature*. https://doi.org/10.1038/s41586-018-0240-x

Choat, B., Jansen, S., Brodribb, T. J., Cochard, H., Delzon, S., Bhaskar, R., Bucci, S. J., Feild, T. S., Gleason, S. M., Hacke, U. G., Jacobsen, A. L., Lens, F., Maherali, H., Martínez-Vilalta, J., Mayr, S., Mencuccini, M., Mitchell, P. J., Nardini, A., Pittermann, J., … Zanne, A. E. (2012). Global convergence in the vulnerability of forests to drought. *Nature*, *491*(7426). https://doi.org/10.1038/nature11688

Cochard, H. (2002). *A technique for measuring xylem hydraulic conductance under high negative pressures*. *25*(6), 815–819. http://doi.wiley.com/10.1046/j.1365-3040.2002.00863.x

Cochard, H., Badel, E., Herbette, S., Delzon, S., Choat, B., & Jansen, S. (2013). Methods for measuring plant vulnerability to cavitation: A critical review. *Journal of Experimental Botany*, *64*(15), 4779–4791. https://doi.org/10.1093/JXB/ERT193

Cochard, H., Barigah, S. T., Kleinhentz, M., & Eshel, A. (2008). Is xylem cavitation resistance a relevant criterion for screening drought resistance among Prunus species? *Journal of Plant Physiology*, *165*(9). https://doi.org/10.1016/j.jplph.2007.07.020

Cochard, H., Delzon, S., & Badel, E. (2015). X-ray microtomography (micro-CT): A reference technology for high-resolution quantification of xylem embolism in trees. *Plant, Cell and Environment*, *38*(1), 201–206. https://doi.org/10.1111/pce.12391

Duursma, R. A., Blackman, C. J., Lopéz, R., Martin-StPaul, N. K., Cochard, H., & Medlyn, B. E. (2019). On the minimum leaf conductance: its role in models of plant water use, and ecological and environmental controls. In *New Phytologist* (Vol. 221, Issue 2, pp. 693–705). Blackwell Publishing Ltd. https://doi.org/10.1111/nph.15395

Franklin, O., Fransson, P., Hofhansl, F., & Joshi, J. (2022). Optimal balancing of xylem efficiency and safety explains plant vulnerability to drought. *BioRxiv*.

Gauthey, A., Peters, J. M. R., Carins-Murphy, M. R., Rodriguez-Dominguez, C. M., Li, X., Delzon, S., King, A., Medlyn, B. E., Tissue, D. T., Brodribb, T. J., & Choat, B. (2020). Evaluating methods used to measure cavitation resistance in seven woody species with differing xylem anatomy: a comparison of visual and hydraulic techniques. *New Phytologist*.

Genard-Zielinski, A. C., Boissard, C., Fernandez, C., Kalogridis, C., Lathière, J., Gros, V., Bonnaire, N., & Ormeño, E. (2015). Variability of BVOC emissions from a Mediterranean mixed forest in southern France with a focus on Quercus pubescens. *Atmospheric Chemistry and Physics*, *15*(1), 431–446. https://doi.org/10.5194/ACP-15-431-2015

Genard-Zielinski, A. C., Boissard, C., Ormeño, E., Lathière, J., Reiter, I. M., Wortham, H., Orts, J. P., Temime-Roussel, B., Guenet, B., Bartsch, S., Gauquelin, T., & Fernandez, C. (2018). Seasonal variations of Quercus pubescens isoprene emissions from an in natura forest under drought stress and sensitivity to future climate change in the Mediterranean area. *Biogeosciences*, *15*(15), 4711–4730. https://doi.org/10.5194/BG-15-4711-2018

Guillemot, J., Martin-StPaul, N. K., Bulascoschi, L., Poorter, L., Morin, X., Pinho, B. X., le Maire, G., R. L. Bittencourt, P., Oliveira, R. S., Bongers, F., Brouwer, R., Pereira, L., Gonzalez Melo, G. A., Boonman, C. C.

F., Brown, K. A., Cerabolini, B. E. L., Niinemets, Ü., Onoda, Y., Schneider, J. V., … Brancalion, P. H. S. (2022). Small and slow is safe: On the drought tolerance of tropical tree species. *Global Change Biology*, *28*(8). https://doi.org/10.1111/gcb.16082

Hartmann, H., Moura, C.F., Anderegg, W.R.L., Ruehr, N.K., Salmon, Y., Allen, C.D., Arndt, S.K., Breshears, D.D., Davi, H., Galbraith, D., Ruthrof, K.X., Wunder, J., Adams, H.D., Bloemen, J., Cailleret, M., Cobb, R., Gessler, A., Grams, T.E.E., Jansen, S., Kautz, M., Lloret, F. and O'Brien, M. (2018), Research frontiers for improving our understanding of drought-induced tree and forest mortality. New Phytol, 218: 15-28. https://doi.org/10.1111/nph.15048

Herbette, S., Charrier, O., Cochard, H., & Barigah, T. S. (2021). Delayed effect of drought on xylem vulnerability to embolism in fagus sylvatica. *Canadian Journal of Forest Research*, *51*(4), 622–626. https://doi.org/10.1139/CJFR-2020-0256/SUPPL_FILE/CJFR-2020-0256SUPPLB.DOCX

Hinckley, T. M., Duhme, F., Hinckley, A. R., & Richter, H. (1980). Water relations of drought hardy shrubs: osmotic potential and stomatal reactivity. *Plant, Cell & Environment*, *3*(2), 131–140. https://doi.org/10.1111/1365-3040.EP11580919

Jinagool, W., Lamacque, L., Delmas, M., Delzon, S., Cochard, H., & Herbette, S. (2018). Is there variability for xylem vulnerability to cavitation in walnut tree cultivars and species (Juglans spp.)? *HortScience*, *53*(2), 132–137. https://doi.org/10.21273/HORTSCI12350-17

La Mantia, T., Cullotta, S., & Garfì, G. (2003). Phenology and growth of Quercus ilex L. in different environmental conditions in Sicily (Italy). *Ecologia Mediterranea*, *29*(1), 15–25. https://doi.org/10.3406/ECMED.2003.1525

Lemaire, C., Quilichini, Y., Brunel-Michac, N., Santini, J., Berti, L., Cartailler, J., Conchon, P., Badel, É., & Herbette, S. (2021). Plasticity of the xylem vulnerability to embolism in Populus tremula x alba relies on pit quantity properties rather than on pit structure. *Tree Physiology*, *41*(8), 1384–1399. https://doi.org/10.1093/TREEPHYS/TPAB018

Lens, F., Picon-Cochard, C., Delmas, C. E. L., Signarbieux, C., Buttler, A., Cochard, H., Jansen, S., Chauvin, T., Doria, L. C., Del Arco, M., & Delzon, S. (2016). Herbaceous Angiosperms Are Not More Vulnerable to Drought-Induced Embolism Than Angiosperm Trees. *Plant Physiology*, *172*(2), 661–667. https://doi.org/10.1104/PP.16.00829

Li, X., Delzon, S., Torres-Ruiz, J., Badel, E., Burlett, R., Cochard, H., Jansen, S., King, A., Lamarque, L. J., Lenoir, N., St-Paul, N. M., & Choat, B. (2020). Lack of vulnerability segmentation in four angiosperm tree species: evidence from direct X-ray microtomography observation. *Annals of Forest Science*, *77*(2). https://doi.org/10.1007/s13595-020-00944-2

Limousin, J. M., Rambal, S., Ourcival, J. M., Rocheteau, A., Joffre, R., & Rodriguez-Cortina, R. (2009). Long-term transpiration change with rainfall decline in a Mediterranean Quercus ilex forest. *Global Change Biology*, *15*(9), 2163–2175. https://doi.org/10.1111/j.1365-2486.2009.01852.x

Limousin, J., Roussel, A., Rodríguez-Calcerrada, J., Torres-Ruiz, J. M., Moreno, M., Jalon, L. G. de, Ourcival, J., Simioni, G., Cochard, H., & Martin-StPaul, N. (2022). Drought acclimation of Quercus ilex leaves improves tolerance to moderate drought but not resistance to severe water stress. *Plant, Cell & Environment*. https://doi.org/10.1111/PCE.14326

Limousin, J.-M. J.-M. J. M., Longepierre, D., Huc, R., & Rambal, S. (2010). Change in hydraulic traits of Mediterranean Quercus ilex subjected to long-term throughfall exclusion. *Tree Physiology*, *30*(8), 1026–1036. https://doi.org/10.1093/treephys/tpq062

Lobo, A., Torres-Ruiz, J. M., Burlett, R., Lemaire, C., Parise, C., Francioni, C., Truffaut, L., Tomášková, I., Hansen, J. K., Kjær, E. D., Kremer, A., Delzon, S., Dahl Kjaer, E., Kremer, A., Delzon, S., Kjær, E. D., Kremer, A.,

& Delzon, S. (2018). Assessing inter- and intraspecific variability of xylem vulnerability to embolism in oaks. *Forest Ecology and Management*, *424*, 53–61. https://doi.org/10.1016/j.foreco.2018.04.031

Machado, R., Loram-Lourenço, L., Farnese, F. S., Alves, R. D. F. B., de Sousa, L. F., Silva, F. G., Filho, S. C. V., Torres-Ruiz, J. M., Cochard, H., & Menezes-Silva, P. E. (2021). Where do leaf water leaks come from? Trade-offs underlying the variability in minimum conductance across tropical savanna species with contrasting growth strategies. *New Phytologist*, *229*(3). https://doi.org/10.1111/nph.16941

Mantova, M., Herbette, S., Cochard, H., & Torres-Ruiz, J. M. (2022). Hydraulic failure and tree mortality: from correlation to causation. *Trends in Plant Science*, *27*(4), 335–345. https://doi.org/10.1016/J.TPLANTS.2021.10.003

Martínez-Vilalta, J., Prat, E., Oliveras, I., & Piñol, J. (2002). Xylem hydraulic properties of roots and stems of nine Mediterranean woody species. *Oecologia*, *133*(1), 19–29. https://doi.org/10.1007/S00442-002-1009-2

Martin-StPaul, N., Delzon, S., & Cochard, H. (2017). Plant resistance to drought depends on timely stomatal closure. *Ecology Letters*, *20*(11), 1437–1447. http://doi.wiley.com/10.1111/ele.12851

Martin-StPaul, N. K., Limousin, J.-M., Vogt-Schilb, H., Rodríguez-Calcerrada, J., Rambal, S., Longepierre, D., & Misson, L. (2013). The temporal response to drought in a Mediterranean evergreen tree: comparing a regional precipitation gradient and a throughfall exclusion experiment. *Global Change Biology*, *19*(8), 2413–2426. https://doi.org/10.1111/gcb.12215

Martin-StPaul, N. K., Longepierre, D., Huc, R., Delzon, S., Burlett, R., Joffre, R., Rambal, S., & Cochard, H. (2014). How reliable are methods to assess xylem vulnerability to cavitation? The issue of "open vessel" artifact in oaks. *Tree Physiology*, *34*(8), 894–905. https://academic.oup.com/treephys/article-lookup/doi/10.1093/treephys/tpu059

Masson-Delmotte, V., Zhai, P., Pörtner, H.-O., Roberts, D., Skea, J., Shukla, P. R., Pirani, A., Moufouma-Okia, W., Péan, C., Pidcock France, R., Connors, S., Matthews, J. B. R., Chen, Y., Zhou, X., Gomis, M. I., Lonnoy, E., Maycock, T., Tignor, M., & Waterfield, T. (2018). Summary for Policymakers. Global Warming of 1.5°C. An IPCC Special Report on the impacts of global warming of 1.5 ºC above pre-industrial levels. In *Global Warming of 1.5°C. An IPCC Special Report on the impacts of global warming of 1.5°C above pre-industrial levels and related global greenhouse gas emission pathways, in the context of strengthening the global response to the threat of climate change,*.

McDowell, N., Pockman, W. T., Allen, C. D., Breshears, D. D., Cobb, N., Kolb, T., Plaut, J., Sperry, J., West, A., Williams, D. G., & Yepez, E. A. (2008). Mechanisms of plant survival and mortality during drought: Why do some plants survive while others succumb to drought? *New Phytologist*, *178*(4), 719–739. https://doi.org/10.1111/j.1469-8137.2008.02436.x

Moreno, M., Simioni, G., Cailleret, M., Ruffault, J., Badel, E., Carrière, S., Davi, H., Gavinet, J., Huc, R., Limousin, J.-M. M., Marloie, O., Martin, L., Rodríguez-Calcerrada, J., Vennetier, M., & Martin-StPaul, N. (2021). Consistently lower sap velocity and growth over nine years of rainfall exclusion in a Mediterranean mixed pine-oak forest. *Agricultural and Forest Meteorology*, *308–309*, 108472. https://linkinghub.elsevier.com/retrieve/pii/S0168192321001556

Moreno, M., Simioni, G., Cochard, H., Doussan, C., Guillemot, J., Decarsin, R., Fernandez-Conradi, P., Dupuy, J.-L., Trueba, S., Pimont, F., Ruffault, J., Jean, F., Marloie, O., & Martin-StPaul, N. K. (2024). Isohydricity and hydraulic isolation explain reduced hydraulic failure risk in an experimental tree species mixture. Plant Physiology, 195(4), 2668–2682. https://doi.org/10.1093/plphys/kiae239

Pivovaroff, A. L., Cook, V. M. W., & Santiago, L. S. (2018). Stomatal behaviour and stem xylem traits are coordinated for woody plant species under exceptional drought conditions. *Plant Cell and Environment*, *41*(11). https://doi.org/10.1111/pce.13367

Pangle, R. E., J. P. Hill, J. A. Plaut, E. A. Yepez, J. R. Elliot, N. Gehres, N. G. McDowell, and W. T. Pockman. 2012. Methodology and performance of a rainfall manipulation experiment in a piñon–juniper woodland. Ecosphere 3(4):28. http://dx.doi.org/10.1890/ES11-00369.1

Poyatos, R., Llorens, P., Piñol, J., & Rubio, C. (2008). Response of Scots pine (Pinus sylvestris L.) and pubescent oak (Quercus pubescens Willd.) to soil and atmospheric water deficits under Mediterranean mountain climate. *Annals of Forest Science*, *65*(3), 1. https://doi.org/10.1051/FOREST:2008003

Rosas, T., Mencuccini, M., Barba, J., Cochard, H., Saura-Mas, S., & Martínez-Vilalta, J. (2019). Adjustments and coordination of hydraulic, leaf and stem traits along a water availability gradient. *New Phytologist*, *223*(2), 632–646. https://doi.org/10.1111/nph.15684

Ruffault, J., Pimont, F., Cochard, H., Dupuy, J.-L., & Martin-StPaul, N. (2022). SurEau-Ecos v2.0: A trait-based plant hydraulics model for simulations of plant water status and drought-induced mortality at the ecosystem level. *Preprint*. https://doi.org/https://doi.org/10.5194/gmd-2022-17

Schindelin, J., Arganda-Carreras, I., Frise, E., Kaynig, V., Longair, M., Pietzsch, T., Preibisch, S., Rueden, C., Saalfeld, S., Schmid, B., Tinevez, J. Y., White, D. J., Hartenstein, V., Eliceiri, K., Tomancak, P., & Cardona, A. (2012). Fiji: An open-source platform for biological-image analysis. In *Nature Methods* (Vol. 9, Issue 7). https://doi.org/10.1038/nmeth.2019

Schneider, C. A., Rasband, W. S., & Eliceiri, K. W. (2012). NIH Image to ImageJ: 25 years of image analysis. In *Nature Methods* (Vol. 9, Issue 7, pp. 671–675). Nature Publishing Group. https://doi.org/10.1038/nmeth.2089

Sergent, A. S., Varela, S. A., Barigah, T. S., Badel, E., Cochard, H., Dalla-Salda, G., Delzon, S., Fernández, M. E., Guillemot, J., Gyenge, J., Lamarque, L. J., Martinez-Meier, A., Rozenberg, P., Torres-Ruiz, J. M., & Martin-StPaul, N. K. (2020). A comparison of five methods to assess embolism resistance in trees. *Forest Ecology and Management*, *468*.

Simioni, G., Marie, G., & Huc, R. (2016). Influence of vegetation spatial structure on growth and water fluxes of a mixed forest: Results from the NOTG 3D model. *Ecological Modelling*, *328*, 119–135. https://www.sciencedirect.com/science/article/pii/S0304380016300205

Sperry, J. S., Hacke, U. G., Oren, R., & Comstock, J. P. (2002). Water deficits and hydraulic limits to leaf water supply. *Plant, Cell and Environment*, *25*(2). https://doi.org/10.1046/j.0016-8025.2001.00799.x

Torres-Ruiz, J. M., Cochard, H., Mayr, S., Beikircher, B., Diaz-Espejo, A., Rodriguez-Dominguez, C. M., Badel, E., & Fernández, J. E. (2014). Vulnerability to cavitation in Olea europaea current-year shoots: Further evidence of an open-vessel artifact associated with centrifuge and air-injection techniques. *Physiologia Plantarum*, *152*(3). https://doi.org/10.1111/ppl.12185

Torres-Ruiz, J. M., Kremer, A., Carins Murphy, M. R., Brodribb, T., Lamarque, L. J., Truffaut, L., Bonne, F., Ducousso, A., & Delzon, S. (2019). Genetic differentiation in functional traits among European sessile oak populations. *Tree Physiology*, *39*(10). https://doi.org/10.1093/treephys/tpz090

Trifiló, P., Raimondo, F., Savi, T., Lo Gullo, M. A., & Nardini, A. (2016). The contribution of vascular and extra-vascular water pathways to drought-induced decline of leaf hydraulic conductance. *Journal of Experimental Botany*, *67*(17). https://doi.org/10.1093/jxb/erw268

Tyree, M. T., & Hammel, H. T. (1972). The measurement of the turgor pressure and the water relations of plants by the pressure-bomb technique. *Journal of Experimental Botany*, *23*(1), 267–282.

Tyree, M. T., & Sperry, J. S. (1988). Do Woody Plants Operate Near the Point of Catastrophic Xylem Dysfunction Caused by Dynamic Water Stress? *Plant Physiology*, *88*(3). https://doi.org/10.1104/pp.88.3.574

Wu, C., Peng, J., Ciais, P., Peñuelas, J., Wang, H., Beguería, S., Andrew Black, T., Jassal, R. S., Zhang, X., Yuan, W., Liang, E., Wang, X., Hua, H., Liu, R., Ju, W., Fu, Y. H., & Ge, Q. (2022). Increased drought effects on the phenology of autumn leaf senescence. *Nature Climate Change 2022 12:10*, *12*(10), 943–949. https://doi.org/10.1038/s41558-022-01464-9